

RESEARCH

Open Access



Cooperative transportation of an object with a nonholonomic constraint by a swarm robot

Yuto Fukao^{1*}, Tatsuro Terakawa¹, Takahiro Endo², Fumitoshi Matsuno³, Yoshihiro Morimoto⁴, Takumi Koshimoto⁴ and Daisuke Mizuno⁴

Abstract

In this paper, we propose a distributed controller for the cooperative transportation of an object with a nonholonomic constraint by a swarm robot. Because an object with passive wheels fixed to it does not slide along the axle direction, its velocity constraint is nonholonomic. We set the center of rotation of the object as a control point of the entire system. To derive the control point of an object with passive fixed wheels, we analyze dynamics of the object. Then we design a distributed cooperative transportation controller considering the nonholonomic constraint of an object with passive fixed wheels based on a kinematic model. We divide the distributed controller into two steps. In the first step, each robot derives the desired velocity and angular velocity of the object to achieve its desired position and orientation. In the second step, each robot calculates its desired velocity to achieve the object's desired velocity and angular velocity. Each robot moves and pushes the object using the distributed controller, and can transport it to the desired position and orientation. We verify the effectiveness of the proposed controller in dynamic simulations and real robot experiments.

Keywords Swarm robotics, Cooperative transportation, Distributed autonomous system, Nonholonomic constraint

Introduction

A swarm robot is a group of many autonomous distributed robots that can cooperate to accomplish tasks that cannot be accomplished by a single robot. The advantages of a swarm robot include scalability, which means that the system does not fail when the number of robots changes; robustness, which means that tasks can be

achieved when some robots fail; and flexibility, which means that the system can adapt to changes in tasks. A swarm robot is expected to be applied in a variety of fields [1]. In this study, we focus on cooperative transport, in which the swarm robot consists of multiple robots that cooperate to transport an object, which makes it possible to transport a heavy object that cannot be transported by a single robot [2].

Various studies have been conducted on the cooperative transportation of an omnidirectionally mobile object by a swarm robot [3–19]. Mainly, two methods exist for cooperative transport by a swarm robot. One is grasping an object using a grasping mechanism [3–7] and the other is pushing an object without using a grasping mechanism [8–19]. In this study, we consider a transport method without a grasping mechanism. This method can be applied to any robot with a mobile function because it

*Correspondence:

Yuto Fukao
fukao.yuto.74m@st.kyoto-u.ac.jp

¹ Department of Mechanical Engineering and Science, Kyoto University, Kyoto, Japan

² Department of Mechanical Engineering, Nagaoka University of Technology, Nagaoka, Japan

³ Department of Electronics and Information Systems Engineering, Osaka Institute of Technology, Osaka, Japan

⁴ Advanced Technology R&D Center, Mitsubishi Electric Corporation, Amagasaki, Japan



© The Author(s) 2025. **Open Access** This article is licensed under a Creative Commons Attribution 4.0 International License, which permits use, sharing, adaptation, distribution and reproduction in any medium or format, as long as you give appropriate credit to the original author(s) and the source, provide a link to the Creative Commons licence, and indicate if changes were made. The images or other third party material in this article are included in the article's Creative Commons licence, unless indicated otherwise in a credit line to the material. If material is not included in the article's Creative Commons licence and your intended use is not permitted by statutory regulation or exceeds the permitted use, you will need to obtain permission directly from the copyright holder. To view a copy of this licence, visit <http://creativecommons.org/licenses/by/4.0/>.

does not require a mechanism to grasp the object; hence, it is highly versatile.

Studies have been conducted on cooperative transportation by a swarm robot without a grasping mechanism by pushing an object in [8–19]. Kube et al. [8, 9] conducted a pioneering study on multiple robots pushing and transporting an object. They adapted the subsumption architecture to cooperative transportation. Cylindrical and rectangular objects were transported in real experiments. Yamada et al. [10] proposed a method in which each robot selected its own action from a set of action options that depended on information such as the position and weight of the neighboring robots and object, and the robots transported a rectangular object. They verified the adaptability of the proposed method to changes to the number of robots and the weight of the object in experiments. Gerkey et al. [11] proposed a method for transporting a rectangular object using two types of robots: a watcher robot and pusher robot. The watcher robot was located in front of the object in the transport direction and the pusher robot was located behind the object. The watcher robot knew the goal position; hence, it sent the desired velocity to pusher robots using communication, and pusher robots pushed the object at the desired velocity. There were significant limitations in the geometry of the applicable object in [8–11].

Fink et al. [12] proposed a method to enable nonholonomic robots to surround and transport a polygonal object in the presence of obstacles. Nonholonomic robots are treated as omni-directional mobile robots by using feedback linearization techniques. The robots maintained the enclosure of the object and transported it. The shape of the transported object was polygonal; hence, the proposed method was highly versatile. The method also generated a trajectory for the object in which the entire robot did not collide with obstacles, and the object was transported along this trajectory. As robots surrounded the object, the method enabled them to transport the object without colliding with obstacles. Chen et al. [13] proposed a method that enables the cooperative transport of an object by pushing the object's surface vertically from a position on the object's surface where the robot could not see the goal. Communication among robots is not used in this method. The proposed method can be applied to any convex object and can transport the object, even if there are not enough robots to surround it, because the object does not need to be surrounded. Researchers have also shown mathematically that the distance from the object to the goal is always reduced using the proposed method. These proposed methods in [12, 13] can be applied to an object of more general geometry than those in [8–11].

Furthermore, Ebel et al. [14, 15] proposed a method for transporting a non-convex polygonal object by

surrounding it with omni-directional mobile robots. In these studies, Ebel et al. determined the optimal transport formation by solving the optimization problem in a distributed manner, which allowed the robots to form the formation that maximized the force and torque from robots to the object, subject to constraints, such as no collisions. In addition, Ebel et al. [16] proposed a method for cooperative transportation using differential-drive mobile robots, achieving distributed transportation of a non-convex polygonal object.

Cooperative transportation methods using evolutionary computation and reinforcement learning have also been proposed. Alkilabi et al. [17, 18] applied controllers obtained by evolutionary computation to real robots to validate the transportation of a rectangular object. Researchers showed that the obtained controllers were robust to the mass and size of the object and scalable to the size of the swarm in real experiments. Shibata et al. [19] proposed a method for acquiring the robot's behavior and transporting an object to the goal using deep reinforcement learning. The shape of the object was a series of hexagons; hence, the shape was complex. When a robot failed, other robots communicated with neighboring robots and generated a new formation to transport the object. Hence, this method is robust against robot failure.

Although studies on cooperative transportation for diverse geometries have been conducted using various approaches, in [8–19], the researchers considered transported objects that could move in all directions. Currently, robots are expected to play an active role in diverse scenarios and environments, such as libraries, shopping malls, airports, and factories. In this context, multiple robots are required to transport bookshelf carts in libraries, shopping carts in shopping malls, luggage carts in airports, trolleys in large event venues, and dollies in factories. Some of these carts have passively moving fixed wheels, which we refer to as passive fixed wheels in this paper. An object with passive fixed wheels has the kinematic constraint that it cannot slide along the axle direction, and this velocity constraint is nonholonomic.

As mentioned above, in previous research methods in which swarm robots cooperatively transported an object by pushing, researchers considered a transported object that could move in all directions. Therefore, conventional methods cannot be applied to objects with two parallel passive fixed wheels because the object cannot move in all directions.

In this study, we consider an object with two parallel passive fixed wheels as the transported object and propose a controller that considers the nonholonomic velocity constraint. The proposed distributed controller

achieves the cooperative transportation of the object by a swarm robot.

Furthermore, our cooperative transportation method involves robots working together to transport objects, meaning that the robots cooperate with each other. However, we do not exchange information with other robots through communication nor sense and utilize their states. In the case of the transportation of the object by multiple robots with communication, communication signals can interfere with each other, potentially leading to improper robot operation. Furthermore, if one of the robots fails and another robot relies on the state of the failed robot, it may move inappropriately. In such cases, the failed robot could disrupt the overall motion of the swarm. Therefore, we do not use the state of any other robot; instead, the proposed controller uses only the absolute position and orientation of the object and the relative position of the robots attached to the object surface from the center of rotation of the object as a control point. In detail, based on the kinematics model of a wheeled object of any shape, each robot determines the desired velocity and angular velocity of the object to reach the desired position and orientation. Next, each robot determines its own desired velocity to achieve the desired velocity and angular velocity of the object in a distributed manner. Thus, each robot can achieve the cooperative transportation of the object by moving according to the obtained desired velocity. Additionally, we verify the effectiveness of the proposed controller by confirming that not only convex but also non-convex objects with passive fixed wheels can be transported to the desired position and orientation in dynamic simulations and real robot experiments.

The paper is organized as follows: We analyze the motion of the arbitrarily shaped transported object and derive a suitable point of the object that is set as a control point in “Control point of an object with passive wheels” section. In “Problem setting” section, we describe the problem statement based on kinematic model. In “Distributed controller” section, we propose the controller for each robot used to transport the object to the desired position and orientation. In “Dynamical simulation” and “Real robot experiment” sections, we present the results of simulations and real robot experiments conducted to verify the effectiveness of the proposed controller, respectively.

Control point of an object with passive wheels

In this section, we determine a control point of an object with two parallel passive fixed wheels during cooperative transportation. A center of rotation of an object is the point about which the object rotates when subjected to an external force. Controlling a point other than the center of rotation results in a moment with respect to

the center of rotation, and the object tends to rotate with respect to the center of rotation, interfering with robots transporting the object. Therefore, we consider the center of rotation as the control point. In order to identify the center of rotation, we analyze the dynamics of a two-dimensional (2D) arbitrarily shaped object with two passive fixed wheels.

We derive the equations of motion of the object. We consider the instantaneous motion of the object and define the coordinate systems at an instant. The coordinate system $\sum_{ob}(o - X'Y')$ is an inertial coordinate system at an instant. The origin o of \sum_{ob} is the position of the middle point between two passive fixed wheels, and the X' -axis of \sum_{ob} is aligned with the direction of the object’s axle as shown in Fig. 1. Let $(x, y)^T$ be the position of the middle point between the wheels with respect to \sum_{ob} and θ be the object’s orientation with respect to the inertial coordinate system $\sum_I(O - XY)$ as shown in Fig. 1. We assume that the object does not slide along the axle direction and that the center of mass is at an arbitrary position in the object. In this paper, we consider the transportation of objects such as carts and trolleys commonly used in daily life, for which the mass and moment of inertia of the wheels are generally negligible compared to those of the main body. Accordingly, the mass and moment of inertia of the wheels are neglected. Let m be the mass of the object, I_c be the moment of inertia around the object’s center of mass, F be the force acting on the object surface with respect to \sum_{ob} , and f_l and f_r be the

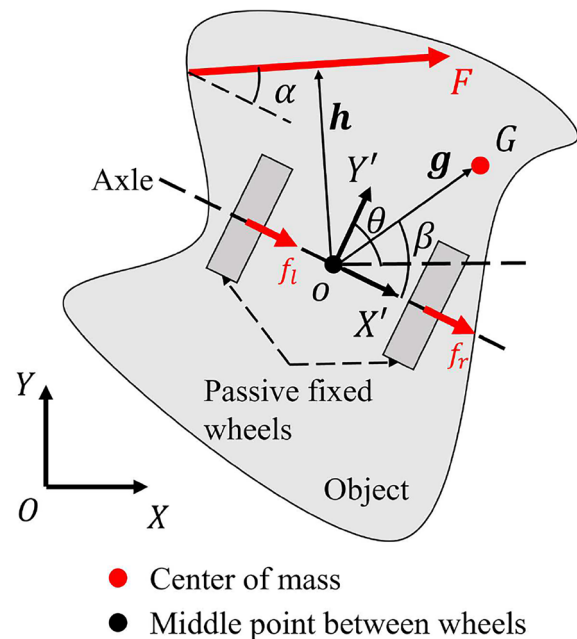


Fig. 1 Object variables for motion analysis of a transported object

forces along the X' -axis acting from the ground to the left and right wheels, respectively, as shown in Fig. 1. Let $\mathbf{g} = (g_x, g_y)^T$ be the vector from o to the center of mass with respect to \sum_{ob} and \mathbf{h} be the moment arm from the middle point between the wheels to F with respect to \sum_{ob} . Let F be the magnitude of F , $g = \sqrt{g_x^2 + g_y^2}$ be the magnitude of \mathbf{g} , h be the magnitude of \mathbf{h} , α be the angle between the X' -axis and F , and β be the angle between the X' -axis and \mathbf{g} . The equations of motion for translation and rotation at the middle point between two wheels are

$$m\ddot{x} = f_l + f_r + F \cos \alpha + mg\ddot{\theta} \sin \beta + mg\dot{\theta}^2 \cos \beta, \tag{1}$$

$$m\ddot{y} = F \sin \alpha - mg\ddot{\theta} \cos \beta + mg\dot{\theta}^2 \sin \beta, \tag{2}$$

$$(I_c + mg^2)\ddot{\theta} = -hF - m\ddot{y}g_x + m\dot{x}g_y. \tag{3}$$

The fourth and fifth term on the right-hand side of (1) and the second and third term on the right-hand side of (2) are inertial force. The second and third terms on the right-hand side of (3) are moment caused by inertial force.

The nonholonomic constraint is that the object cannot slide along the axle direction and is defined as

$$\dot{x} = 0. \tag{4}$$

Substituting $g_x = g \cos \beta, g_y = g \sin \beta$, and (4) into (1), (2), and (3), we obtain

$$0 = f_l + f_r + F \cos \alpha + mg_y\ddot{\theta} + mg_x\dot{\theta}^2, \tag{5}$$

$$m\ddot{y} = F \sin \alpha - mg_x\ddot{\theta} + mg_y\dot{\theta}^2, \tag{6}$$

$$(I_c + mg^2)\ddot{\theta} = -hF - mg_x\ddot{y}. \tag{7}$$

Furthermore, substituting (6) into (7), we obtain

$$(I_c + mg^2)\ddot{\theta} = -(h + g_x \sin \alpha)F + mg_x^2\ddot{\theta} - mg_x g_y \dot{\theta}^2. \tag{8}$$

Then, using $g^2 = g_x^2 + g_y^2$, we derive

$$(I_c + mg_y^2)\ddot{\theta} = -(h + g_x \sin \alpha)F - mg_x g_y \dot{\theta}^2. \tag{9}$$

Finally, we derive the object's center of rotation to be controlled. To this end, we describe the physical meaning of the obtained equation of motion of rotation (9). We define point P (blue dot in Fig. 2) as $(g_x, 0)^T$ with respect to \sum_{ob} , and point Q as the cross point of F and its perpendicular line passing through P , as shown in Fig. 2. The red dashed line in Fig. 2 represents a straight

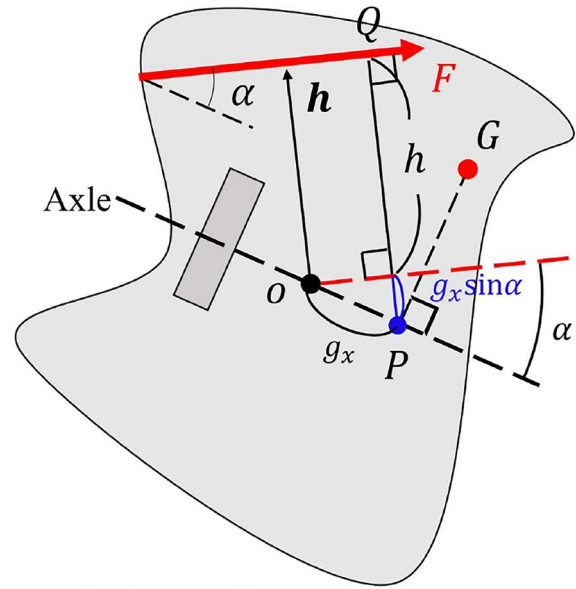


Fig. 2 Position of the object's center of rotation

line parallel to F passing through o . First, the left-hand side of (9) is the moment of inertia around the blue point P . We consider the first term of right-hand side of (9). Figure 2 shows the distance of the perpendicular line from P to F as $h + g_x \sin \alpha$ geometrically, where h is the distance from Q to the red dotted line, and $g_x \sin \alpha$ is the distance from P to the red dotted line. This corresponds to the first term of right-hand side of (9). It means that the first term of right-hand side of (9) represents the moment around P caused by F . Next, we consider the second term of the right-hand side of (9). The expression $mg_x g_y \dot{\theta}^2$ can be rewritten as $g_x \sin \beta \times mg\dot{\theta}^2$. Here, $mg\dot{\theta}^2$ regards as the centripetal force acting from G toward o , while $g_x \sin \beta$ corresponds to the moment arm from P to the centripetal force $mg\dot{\theta}^2$. Therefore, the second term of the right-hand side of (9) represents the moment around P caused by the centripetal force $mg\dot{\theta}^2$.

Therefore, we can regard the equation of motion of rotation obtained as the equation of motion of rotation around P , and we can clarify that P is the center of rotation of the object. Then, the obtained point P is defined as the control point. In the next section, we consider the problem of controlling the center of rotation P and transporting the object.

Problem setting

In this section, we set up the problem statement of the cooperative transportation of an object with two parallel passive fixed wheels by a swarm robot. We consider a 2D environment with no obstacles as the environment in which the robots transport the object. There is one object and n robots in the environment, and the robots are attached to the object’s surface. We consider cooperative transportation of an object by a swarm robot, specifically in the situation where there are enough robots to surround the object. Therefore, we assume that form closure is achieved by the robots surrounding the object, as shown in Fig. 3. Form closure is a geometric constraint that fixes the degrees of freedom of movement of an object, and represents the inability of the object to perform translational and rotational movements in the robot’s enclosure, as defined in [20]. In order to enhance the resultant force applied to the object by the robots during transportation, it is desirable to locate more robots on the side opposite to the direction of the object’s motion while maintaining form closure. However, since this study is based on a kinematic model, forces interactions are not considered. Therefore, it should be noted that the proposed method does not discuss the optimal positioning of robots in order to apply large pushing forces, which remains an issue to be addressed in future work. There may be situations in which the object needs to move in reverse during transportation. In such cases, the robots that were positioned on the forward side during forward movement become responsible for pushing the object in reverse. An advantage of the proposed

method is that the robot formation does not need to be altered, even when the direction of motion changes. However, a drawback is that some robots do not contribute to object pushing at all times, despite being necessary for preserving form closure. Consequently, when there is a possibility that the object need to switch between forward and backward motion, it is not always optimal to place as many robots as possible on the side opposite to the direction of the object’s motion in the initial state. The minimum number of robots is determined by the smallest number required to achieve form closure. If the number of robots falls below this threshold, form closure cannot be established, and thus the object cannot be transported. The maximum number of robots is defined by the number of robots when the object is completely surrounded without any gaps between robots. If the number of robots exceeds that limit, some robots may fail to attach to the object’s surface. We assume that the robot is omni-directional and only control the position of the center of the robot. As the object has passive fixed wheels, it does not slide along the axle direction, and its velocity constraint is nonholonomic. We assume that the object’s center of mass exists at an arbitrary position in the object.

We define the inertial coordinate system $\sum_I(O - XY)$, as shown in Fig. 3. The position of the robot i with respect to \sum_I is denoted by p_i . We consider controlling the center of rotation, which was derived in “Control point of an object with passive wheels” section. The position of the object’s center of rotation P is defined as $(p_x, p_y)^T$ with respect to \sum_I , and the absolute angle between the X -axis and the object’s direction of translation with respect to \sum_I is θ . The direction of translation of the object is denoted by the unit vector $e_o = (\cos \theta, \sin \theta)^T$. As shown in Fig. 3, the robots are attached to the surface of the object, and the vector from the object’s center of rotation P to robot i is denoted by r_i with respect to \sum_I . In this study, we consider kinematic models of the robot and object. The kinematic equation for robot i is given by

$$\dot{p}_i = u_i, \tag{10}$$

where u_i is the input velocity command of robot i . Additionally, the kinematics equation of the object is

$$\frac{d}{dt} \begin{pmatrix} p_x \\ p_y \\ \theta \end{pmatrix} = \begin{pmatrix} \cos \theta & 0 \\ \sin \theta & 0 \\ 0 & 1 \end{pmatrix} \begin{pmatrix} v \\ \omega \end{pmatrix}, \tag{11}$$

where v is the object’s velocity in the translational direction and ω is the object’s angular velocity.

We assume that the robots know the position of the object’s axle and its center of mass. We consider transporting a predefined object, such as shopping cart in a

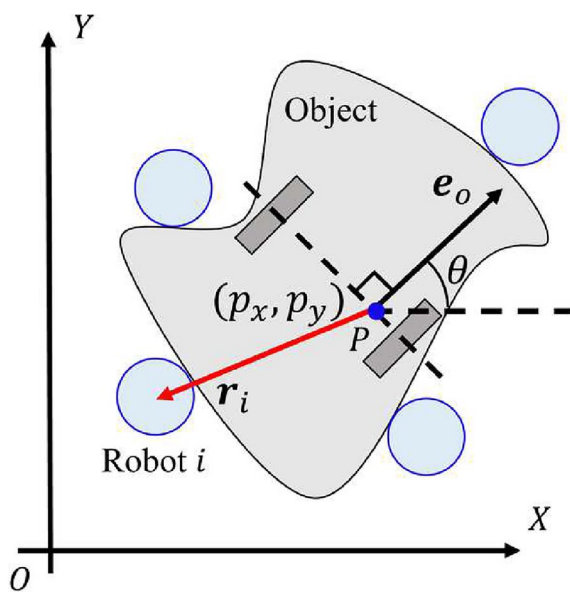


Fig. 3 Variable definitions of robots and an object

shopping mall or a bookshelf cart in a library. Since the robots can obtain the position of the axle and the center of mass from its camera information by using image recognition technology, we consider this assumption reasonable in situations such as shopping malls and libraries. However, in scenarios where multiple loads are placed on an object, it might be challenging for robots to obtain the center of mass solely from their camera information. To overcome this, we consider employing a method similar to that in [21], where a robot pushes an object to determine its center of friction, which could enable robots to obtain the object's center of mass. By obtaining the position of the object's axle and its center of mass, each robot can determine the center of rotation and acquire the object's position p_x, p_y and orientation θ , and the robot's own attached position r_i with respect to \sum_I . Moreover, since the robots do not need information from other robots, communication among robots is not required.

The control objective is to find the input velocity command u_i of robot i to make the object's position p_x, p_y and orientation θ converge to 0.

Distributed controller

In this section, we discuss a distributed controller used by a robot to achieve the desired position and orientation of an object with passive fixed wheels. Each robot calculates only its own input according to the proposed distributed controller. As previously mentioned, the proposed method assumes that the robots have achieved form closure with respect to the object. First, we describe the concept of the design of the controller.

Let us consider multiple points fixed on the object's surface. When the object moves with velocity v and angular velocity ω , we assume that the point i fixed on the object's surface moves with a velocity vector v_i . Conversely, if multiple points fixed on the object's surface move with velocity v_i , the object itself can move with velocity v and angular velocity ω . If we consider these points on the object's surface as positions of robots, and they move with the previously given velocity v_i , they can transport the object with velocity v and angular velocity ω . Assuming that the robots achieve form closure by surrounding the object, the object becomes fixed relative to the robot enclosure and it moves along with the robot enclosure. This is an outline of the concept of the proposed distributed controller.

We divide the robot's controller into two steps. To obtain desired motion of the object with two parallel passive wheels, the object is regarded as a vehicle with two active wheels and derive the desired velocity and angular velocity of the object by using existing controllers on controlling two-wheeled vehicles with nonholonomic constraints. Vehicle control research typically focuses

on finding the desired velocity and angular velocity of a vehicle with active wheels to achieve a desired position and orientation. In this study, as the object has passive wheels and cannot move actively, the movement of the object is achieved through motion of robots that are attached to the object surface. In the second step, each robot calculates its desired velocity to achieve the object's desired velocity and angular velocity, which were given in the first step. We describe the details of each step in the following subsection.

Step 1: Object's desired velocity and angular velocity

In this step, we aim to find the desired velocity and angular velocity of the object to reach the desired position and orientation. Let v_d and ω_d denote the object's desired velocity and angular velocity, respectively. To design v_d and ω_d , we use the existing control method on controlling two-wheeled vehicles with nonholonomic constraints to the desired position and orientation. Several control methods exist for such a nonholonomic system, including time-axis state control [22], time-varying state feedback control [23, 24], and discontinuous feedback control [25]. For our study, we use the method proposed by Khennouf and Canudas [25], which guarantees exponential convergence to the desired position and orientation. We design v_d and ω_d as follows:

$$\begin{aligned} v_d &= (-k_1 p_x - k_2 s \tan \theta / V) / \cos \theta, \\ \omega_d &= (-k_1 \tan \theta - k_2 s p_x / V) \cos^2 \theta, \end{aligned} \quad (12)$$

where $V = p_x^2 + \tan^2 \theta$, $s = p_y - 1/2 p_x \tan \theta$, and k_1, k_2 represent control gains. This controller is designed to ensure the exponential convergence of $V(t)$ and $s(t)$. When V and s are zero, p_x, p_y , and θ also become zero, so the position and orientation converge to the desired position and orientation. The first term of (12) contributes to the convergence of V , and the second term of (12) facilitates the convergence of s . Actual robots have limitations on the forces and torques they can exert. Therefore, dynamic simulations are conducted in advance to determine the control gains k_1 and k_2 such that the control inputs v_d and ω_d for the robots do not exceed their output capabilities. If the object can move with its desired velocities v_d and ω_d , the object can reach the desired position and orientation.

Step 2: Robot's desired velocity

In this step, we propose a controller that makes the robots attached to the object's surface achieve the desired velocity v_d and ω_d of the object obtained in the first step through their motion. If the robots achieve the motion, it means that the robots can push the object with the desired velocity. We assume that the robots are attached to the object's surface and achieve form closure. First, we

consider the scenario in which the robot is fixed to the object's surface and the object is moving with velocity v and angular velocity ω . Let r_i represent the relative position of robot i fixed on the object's surface as shown in Fig. 3. The velocity v_i of robot i at position r_i is given by $v_i = v e_o + \omega e_z \times r_i$, where e_z is the unit vector perpendicular to the X and Y -axes of the inertial coordinate system \sum_I . Conversely, if form closure is achieved by the robot's enclosure around the object and robot i attached to the object moves with velocity $v_i = v e_o + \omega e_z \times r_i$, then the object can be transported with velocity v and angular velocity ω . Therefore, we design the velocity command u_i of robot i to achieve the desired velocity v_d and ω_d of the object as follows:

$$u_i = v_d e_o + \omega_d e_z \times r_i. \tag{13}$$

From (12), we can calculate v_d and ω_d based on the positions p_x and p_y , and the orientation θ of the object, which can be measured by each robot i . We can compute e_o based on θ , and $e_z = [0, 0, 1]^T$ is given. Because u_i can be given by each robot i , the control law (13) represents a distributed controller.

However, in the real situation, the robots' velocities could not reach the velocity command because of the velocity errors of the actual robots, the limitations on their force and torque output, and reaction forces from the object or ground to the robots; hence, closure by surrounding robots might not be accomplished. Thus, we included PD feedback controller to keep the robot in its initial position on the object's surface.

We define robot's initial position on the object's surface as p_{id} , velocity of the robot's initial position on the object's surface as \dot{p}_{id} , the vector from P to robot's initial position on the object's surface as r_{id} , and the vector from the current robot's position to the robot's initial position on the object's surface as $s_i := p_{id} - p_i$, as shown in Fig. 4. Here, \dot{p}_{id} is expressed as $\dot{p}_{id} = v_d e_o + \omega_d e_z \times r_{id}$. Adding a PD feedback control to (13) to keep the robot in its initial position on the object's surface yields the modified velocity command as follows.

$$u_i = \dot{p}_{id} + k_p(p_{id} - p_i) + k_v(\dot{p}_{id} - \dot{p}_i), \tag{14}$$

where k_p and k_v are positive control gains. Substituting (14) into (10) and rearranging in terms of s_i , we obtain

$$k_p s_i + (1 + k_v) \dot{s}_i = 0, \tag{15}$$

which implies that s_i converges exponentially to zero.

The exponential convergence of the controller in Step 1 is guaranteed by the method proposed by Khennouf et al. [25], which is applied in Step 1. Once the object reaches the desired velocity and angular velocity obtained in Step 1 using [25], its position and orientation converge. In

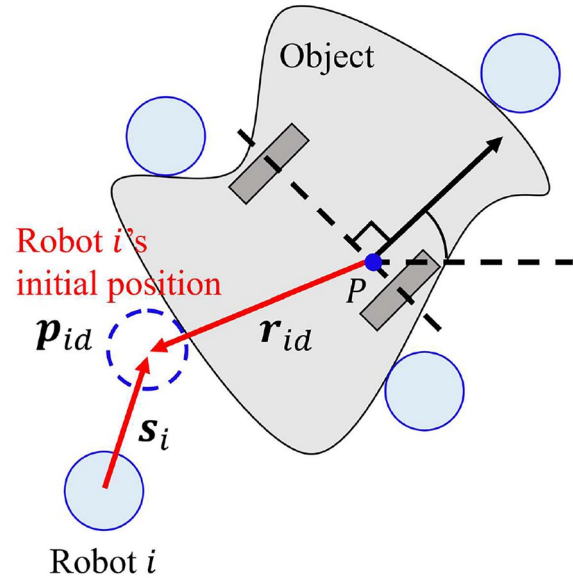


Fig. 4 Feedback to the object's surface

Step 2, the proposed controller drives the robots so that the object can realize the desired velocity and angular velocity found in Step 1. Therefore, the overall controller ensures convergence.

Dynamical simulation

We verified the effectiveness of the proposed controller using the dynamics simulator *OpenDynamicsEngine*. In particular, to demonstrate the effectiveness of the proposed controller in multiple cases with different settings, we conducted two types of simulations. Each simulation involved different numbers of robots, different object shapes, and different initial positions of objects.

Simulation 1

In this simulation, 15 robots transported a concave object with two passive fixed wheels to a desired position and orientation. The geometry of the robot was a cylinder with parameters of radius 0.1 m, height 0.15 m, and mass 3.0 kg. The transported object consisted of a base, two parallel passive fixed wheels, and a ball caster. The base was a J-shaped concave object, as shown in Fig. 5. The parameters of the base were the length of the top edge 2.1 m, the length of the left edge 1.0 m, the length of the bottom edge 1.8 m, the width 0.3 m, and the height 0.05 m, and mass 10.0 kg. The parameters of the wheel were radius 0.05 m and mass 1.0 kg, and the parameters of the ball caster were radius 0.05 m and mass 1.0 kg. Two passive fixed wheels are mounted parallel to the base's bottom at the top and bottom edges, and a ball caster is mounted at the left edge. The center of rotation of the

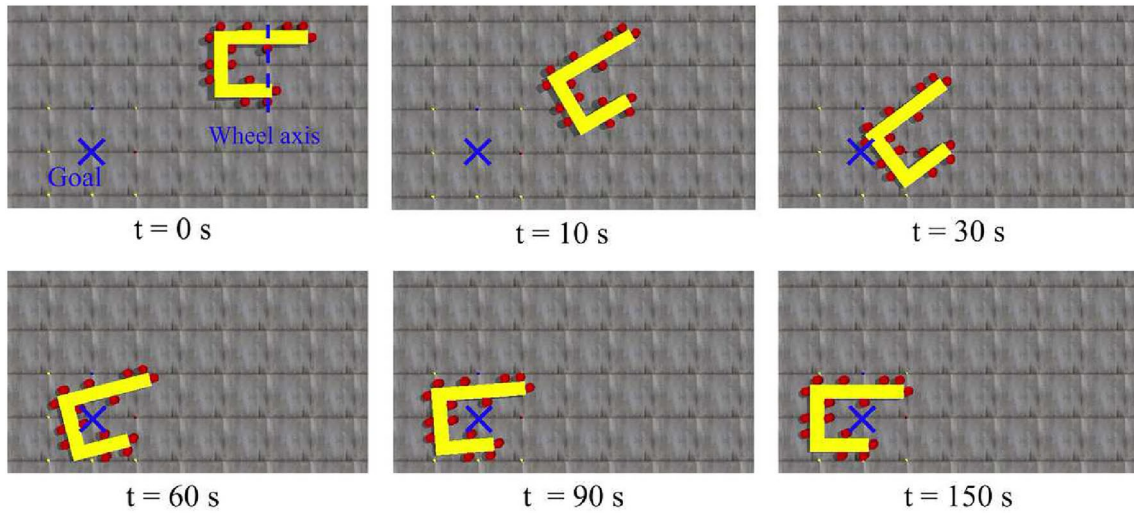


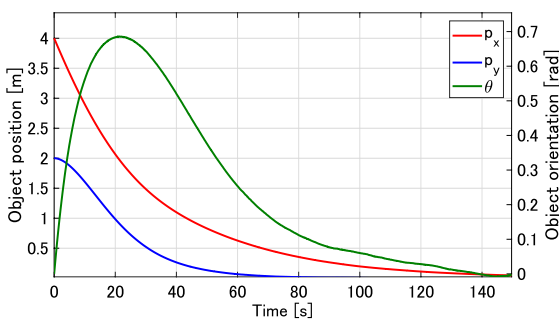
Fig. 5 Snapshot of Simulation 1 results of the cooperative transport of a J-shaped concave object by 15 robots

object was offset from the middle point between the two passive fixed wheels by 0.038 m in the axle direction and 0.375 m in the direction of travel.

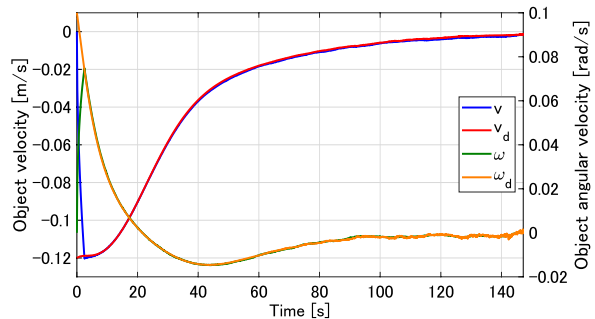
The coefficient of friction between the object’s base and the robot was set as 0.1, and the coefficient of friction between the object’s caster and the ground was 0.1. We set the coefficient of friction between the object’s wheels and the ground to infinity to prevent sliding along the axle direction. We set the position and orientation of the object’s center of rotation in the initial state to $p_x(0) = 4$ m, $p_y(0) = 2$ m, and $\theta(0) = 0$ deg in the inertial coordinate system, and set the object’s desired position and orientation to $p_{xd} = 0$ m, $p_{yd} = 0$ m, and $\theta_d = 0$ deg. The initial positions of the 15 robots at $t = 0$ s are shown in Fig. 5. If the object’s position, orientation, velocity, and angular velocity satisfied the following conditions for 5 s, we defined the task as complete: $-0.01 < p_x, p_y < 0.01, -0.005 < \theta < 0.005, -0.001 < v, \omega < 0.001$.

We set the control gains as follows: $k_1 = 0.03, k_2 = 0.1, k_p = 0.2$, and $k_v = 0.1$.

The simulation result with the above settings is shown in Fig. 5. As shown in Fig. 5, the robots pushed the object to achieve the translational and rotational motion of the object, and transported it to the desired position and orientation. Figure 6a shows the positions p_x and p_y , and the orientation θ of the object, which indicates that they converged to 0. Therefore, the position and orientation of the object’s center of rotation reached the desired position and orientation. This means that the control objective was achieved and the effectiveness of the proposed controller was confirmed. Figure 6b shows the velocity and desired velocity of the object, and the angular velocity and desired angular velocity of the object. We found that the object was transported by achieving the desired velocities.



(a) Object’s position and orientation in Simulation 1



(b) Object’s velocity and angular velocity in Simulation 1

Fig. 6 Object’s states in Simulation 1

As shown in Fig. 6b, the object's velocity and angular velocity could not reach the desired velocities until $t = 3$ s. This simulation was dynamical; hence, it took time to reach the desired velocities because of the inertial effect of the object.

Simulation 2

In this simulation, 10 robots transported a concave object with two parallel passive fixed wheels to a desired position and orientation. The robots and the simulation environment utilized were identical to those used in Simulation1. The base of the transported object was a H-shaped concave object, as shown in Fig. 7. The parameters of the base were the length of the top edge 1.8 m, the length of the middle edge 0.9 m, the length of the bottom edge 1.0 m, the width 0.3 m, and the height 0.05 m, and mass 10.0 kg. The center of rotation of the object was offset from the middle point between the two passive fixed wheels by 0.038 m in the axle direction.

We set the position and orientation of the object's center of rotation in the initial state to $p_x(0) = 5$ m, $p_y(0) = -3$ m, and $\theta(0) = 0$ deg in the inertial coordinate system, and set the object's desired position and orientation to $p_{xd} = 0$ m, $p_{yd} = 0$ m, and $\theta_d = 0$ deg. The initial positions of the 10 robots at $t = 0$ s are shown in Fig. 7.

The simulation result with the above settings is shown in Fig. 7, the position and orientation of the object are shown in Fig. 8a, and the object's velocity and angular velocity are shown in Fig. 8b. From these figures, it is shown that the proposed controller successfully

transported the H-shaped object to the desired position and orientation. Therefore, the proposed method works effectively even when the number of robots, object's shape, and initial position of an object are changed.

Real robot experiment

To verify the effectiveness of the proposed controller, we conducted two kinds of experiment using real robots. In the first experiment, we conducted an experiment in which four robots cooperatively transport an object, and the results were compared with the results of a dynamical simulation conducted under the same conditions. In the second experiment, we conducted an experiment in which six robots cooperatively transport an object, and verified the robustness and scalability of the proposed method by decreasing and increasing the number of robots during the transportation.

Experiment and comparison with simulation

In the experiment, we used four robots to transport an object with two parallel passive fixed wheels to a desired position and orientation.

We configured the experimental system as shown in Fig. 9. We acquired the positions p_x and p_y , and the orientation θ of the object, and the position of the robot using motion capture. We sent the data acquired using motion capture to the control PC via LAN and the control PC calculated the velocity input command u_i for each robot. The control PC then sent the calculated input u_i to each robot via Bluetooth communication. Although the experimental system was centralized, it was appropriate

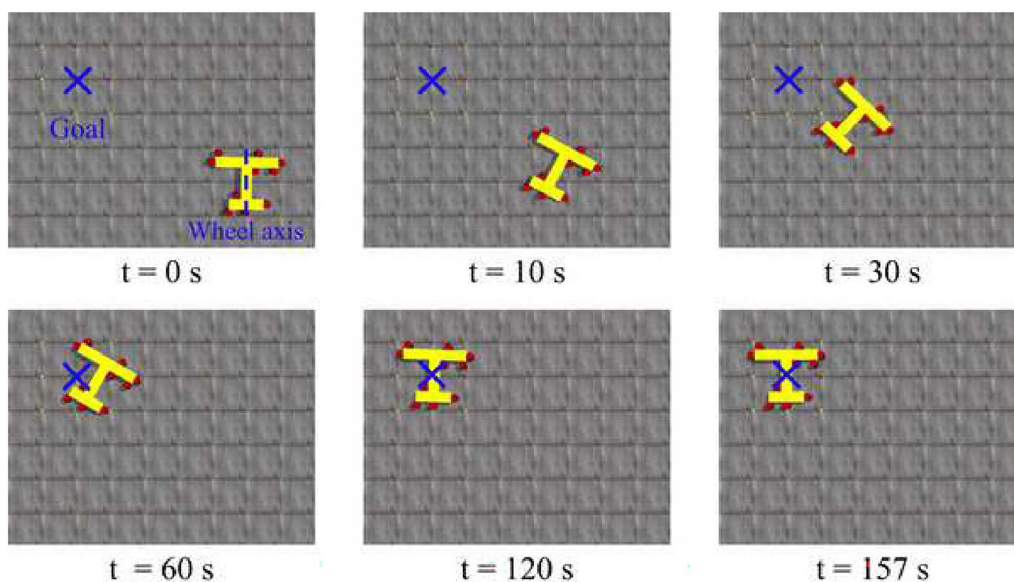
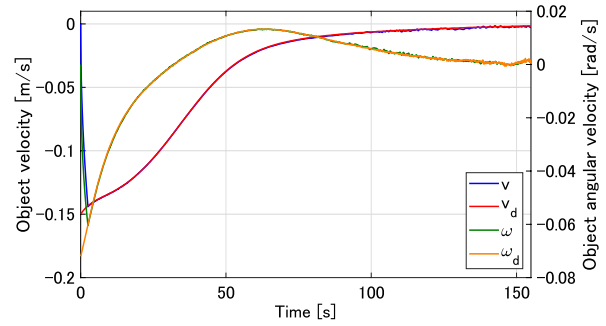
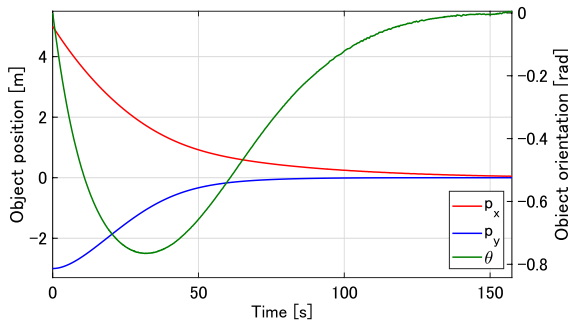


Fig. 7 Snapshot of Simulation 2 results of the cooperative transport of a H-shaped concave object by 15 robots



(a) Object's position and orientation in Simulation 2

(b) Object's velocity and angular velocity in Simulation 2

Fig. 8 Object's states in Simulation 2

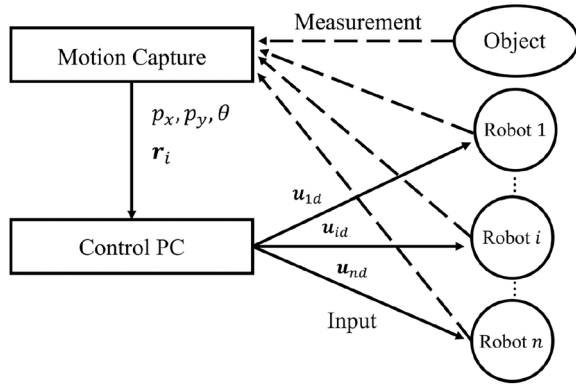
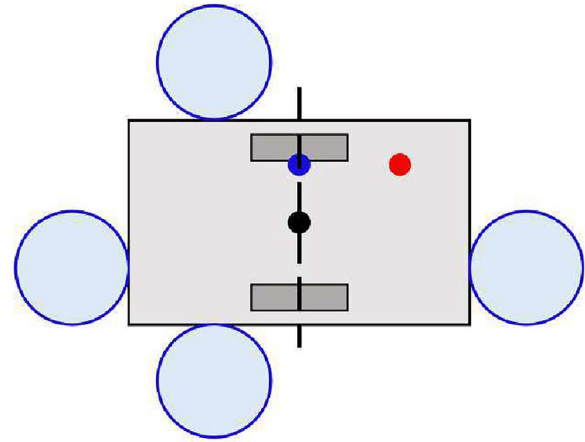


Fig. 9 Outline drawing of the experimental system



- Center of mass
- Middle point between wheels
- Center of rotation

Fig. 10 Initial scenario in the experiment

as a verification experiment because we implemented the proposed controller in a distributed manner.

The robot was a 3WD48mm omni-wheel robot from Vstone corporation that could independently control its position and orientation, and could move in any direction on a 2D plane. The robot was enclosed by a circular cover, which gave it a circular shape with a radius of 0.125 m and mass of 1.5 kg. The transported object consisted of a base, passive stationary wheels, and ball casters, and we placed weight on the base to offset the center of rotation from the middle point between the wheels. The base was a rectangular object with a base side length of 0.5 m × 0.3 m. We fixed the two parallel passive fixed wheels at the center of the base and attached four free-rotating ball casters at each corner of the base. The mass of the object was 1.5 kg, and because we placed a 1.16 kg weight on the object, the center of rotation of the object was offset from the middle point between the two passive fixed wheels by 0.03 m in the axle direction and 0.07 m in the direction of travel, as shown in Fig. 10. We calculated the offset displacement using CAD software.

We set the initial state of the object to $p_x(0) = 4.0$ m, $p_y(0) = 2.0$ m, and $\theta(0) = 1.0$ rad in the inertial coordinate system, and set the desired state of the object to $p_{xd} = 0$ m, $p_{yd} = 0$ m, and $\theta_d = 0$ rad. We set the initial position of each robot as shown in Fig. 10. When the object's position, orientation, velocity, and angular velocity satisfied the following conditions for 5 s, we defined the task as complete: $-0.05 < p_x, p_y < 0.05$, $-0.03 < \theta < 0.03$, $-0.001 < v, \omega < 0.001$. We set the control gains as follows: $k_1 = 0.03$, $k_2 = 0.1$, $k_p = 0.2$, and $k_v = 0.1$.

The snapshot of experimental results is shown in Fig. 11. The figure shows that each robot pushed the

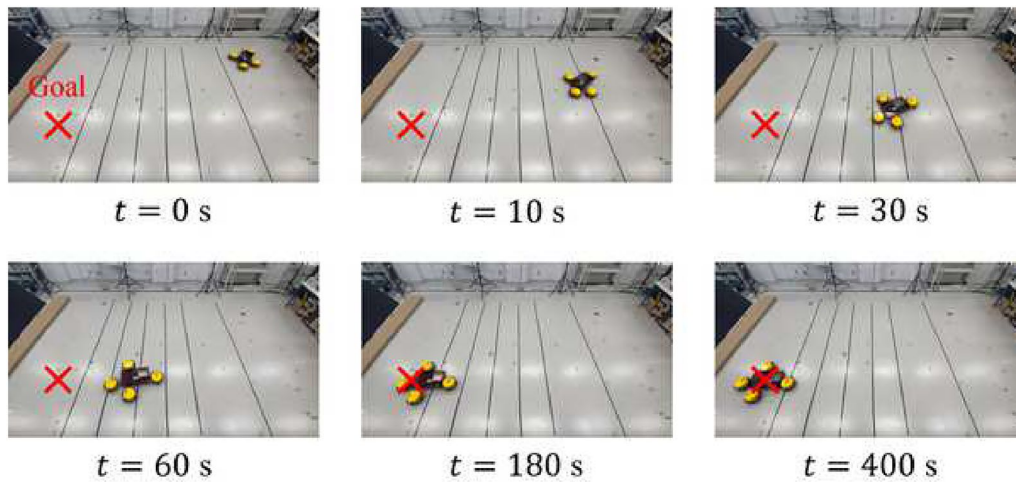


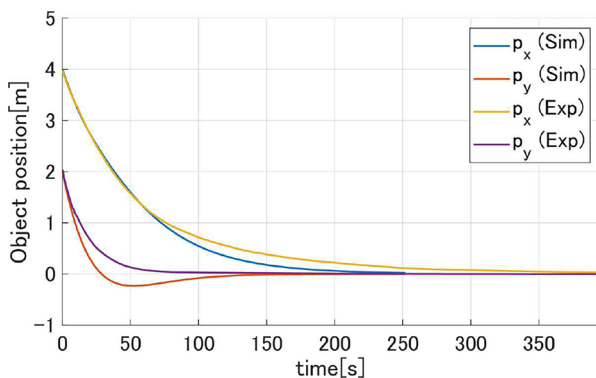
Fig. 11 Snapshot of the experimental results of the cooperative transportation of the object by four robots

object with passive fixed wheels and transported it to the desired position and orientation. Thus, we demonstrated that the method was effective, even for an object with a center of rotation different from the middle point between the wheels.

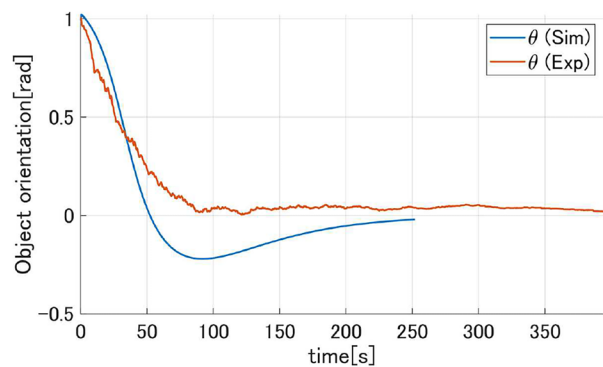
Additionally, we conducted dynamic simulations using the same parameter settings as the real robot experiment. The results of the simulation are presented in Figs. 12 and 13, along with the results of the real robot experiment. Figure 12a shows the position p_x, p_y of the object, which indicates that the object reached the desired position. Figure 12b shows the object’s orientation θ , which indicates that the object reached the desired orientation in both the simulation and experiment. We compared the simulation with the real robot experiment, which

indicated that the real robot experiment took longer to converge. In the experiment, there are difference of friction, viscosity, dead-zone, and other factors that cannot be taken into account in the simulation, possibly causing the difference between the experimental and simulation results.

Figure 13a shows the velocity and desired velocity of the object, which indicates that the velocity followed the desired velocity. Figure 13b shows the angular velocity and desired angular velocity of the object, which indicates that the angular velocity followed the desired angular velocity. The angular velocity result in the real robot experiment was more vibratory than that in the simulation. This phenomenon is considered to have occurred because the robots could not accomplish form closure

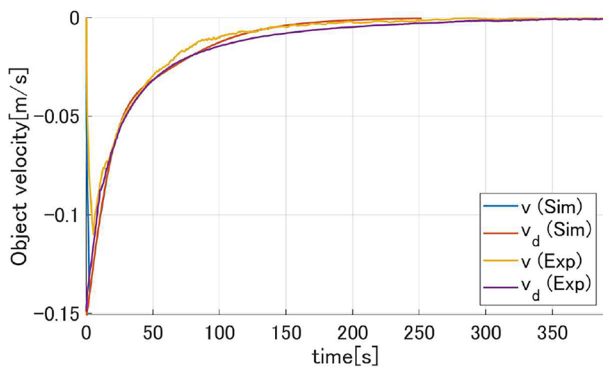


(a) Object’s position in the simulation and the experiment

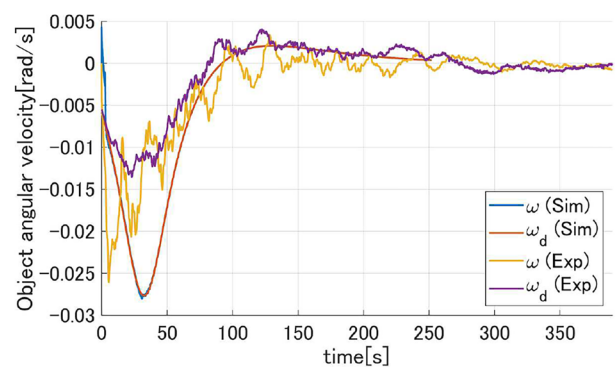


(b) Object’s orientation in the simulation and the experiment

Fig. 12 Object’s position and orientation in the simulation and the experiment



(a) Object's velocity in the simulation and the experiment



(b) Object's angular velocity in the simulation and the experiment

Fig. 13 Object's velocity and angular velocity in the simulation and the experiment

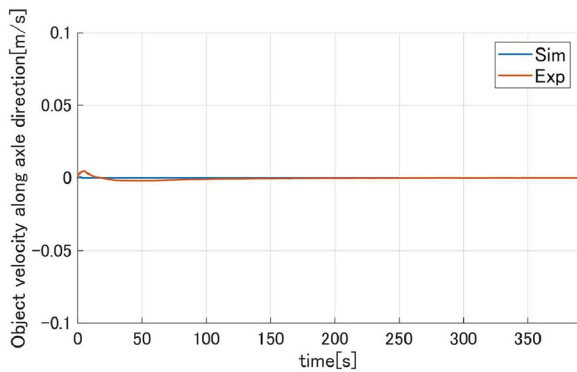


Fig. 14 Object's velocity along the axle direction in the simulation and the experiment

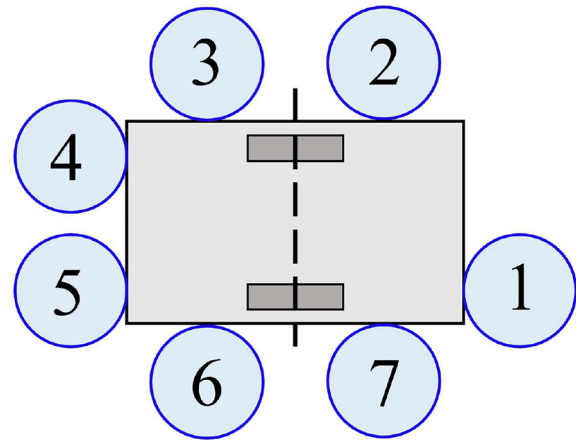


Fig. 15 Robot's location in the experiment

away from the object, which allowed the object to move freely within the robot's closure.

Additionally, Fig. 14 represents the velocity along the axle direction of the object. Since the velocity along the axle direction of the object is sufficiently small, it can be confirmed that the nonholonomic constraint is satisfied.

Compared to the dynamic simulation in "Dynamical simulation" section, the number of robots used in the simulation and the experiment were different, and the proposed method accomplished the transportation even if the number of robots was different, demonstrating the scalability of the proposed method. Also, the shape of the object to be transported in the simulation and the experiment was different, and the proposed method achieved transport even when the shape of the object was different, indicating the flexibility of the proposed method.

Experiment with varying numbers of robots

We conducted an experiment in which six robots cooperatively transport an object, and we verified the

robustness and scalability of the proposed method by decreasing and increasing the number of robots during the transportation. Two robots were removed during transport, and one robot was added at a new location. The experimental system, the robots and the object used in the experiment are the same as in "Experiment and comparison with simulation" section. We set the initial state of the object to $p_x(0) = 3.0$ m, $p_y(0) = 2.0$ m, and $\theta(0) = 1.0$ rad in the inertial coordinate system, and set the desired state of the object to $p_{xd} = 0$ m, $p_{yd} = 0$ m, and $\theta_d = 0$ rad. For explanation, we number the locations around the object as shown in the Fig. 15. At the initial state $t = 0$ s, six robots located at 1, 3, 4, 5, 6, 7 in the Fig. 15. During the experiment, the robots at 4 and 7 were removed at $t = 30$ s and new one robot was added at a new location 2 at $t = 60$ s. When the object's position, orientation, velocity, and angular velocity satisfied the fol-

lowing conditions for 5 s, we defined the task as complete: $-0.05 < p_x, p_y < 0.05, -0.02 < \theta < 0.02, -0.001 < v, \omega < 0.001$.

As shown in Fig. 16 at $t = 40$ s, we can see that two robots were removed and four robots transported the object, and at $t = 70$ s, we can see that one robot is added to the new location and five robots transported the object.

Figure 17 shows the states of the object, which indicates that the object reached the desired position and orientation, even if the number of robots decreases or increases during transportation, or if the robots' locations change during transportation. Therefore, we

verified the robustness and scalability of the proposed method. However, this method cannot consider the case where robots break down and interfere with the progress of other robots or objects, or where form closure is not achieved, so these issues are future work.

Additionally, Fig. 18 shows the velocity of the object along the axle direction. As this velocity is sufficiently small, it confirms that the nonholonomic constraint is satisfied.

Furthermore, in order to verify the adaptability of the proposed method to variations in initial conditions, additional experiments were conducted with different initial

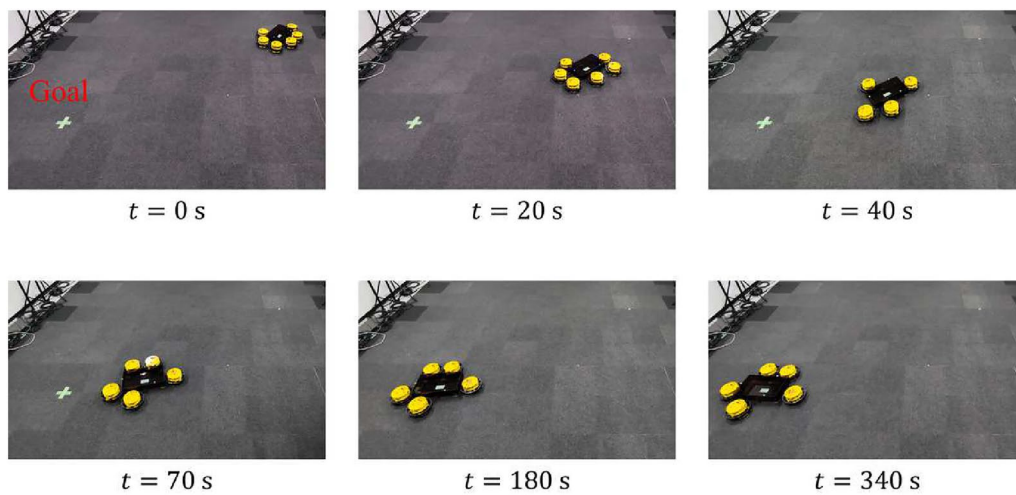


Fig. 16 Snapshot of the experimental results of the cooperative transportation of the object by six robots. The number of robots is increasing or decreasing during transportation

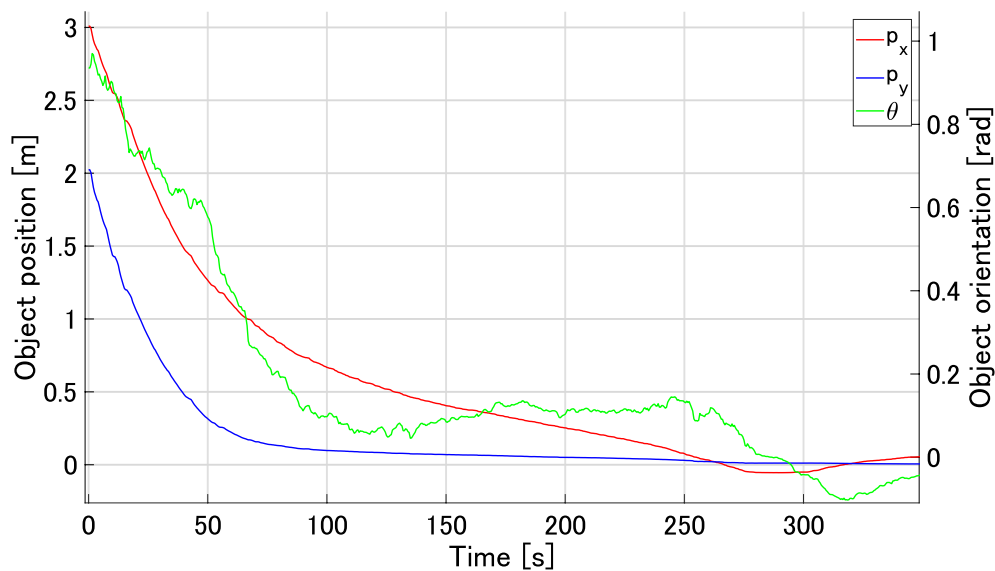


Fig. 17 Object's position and orientation in the experiment

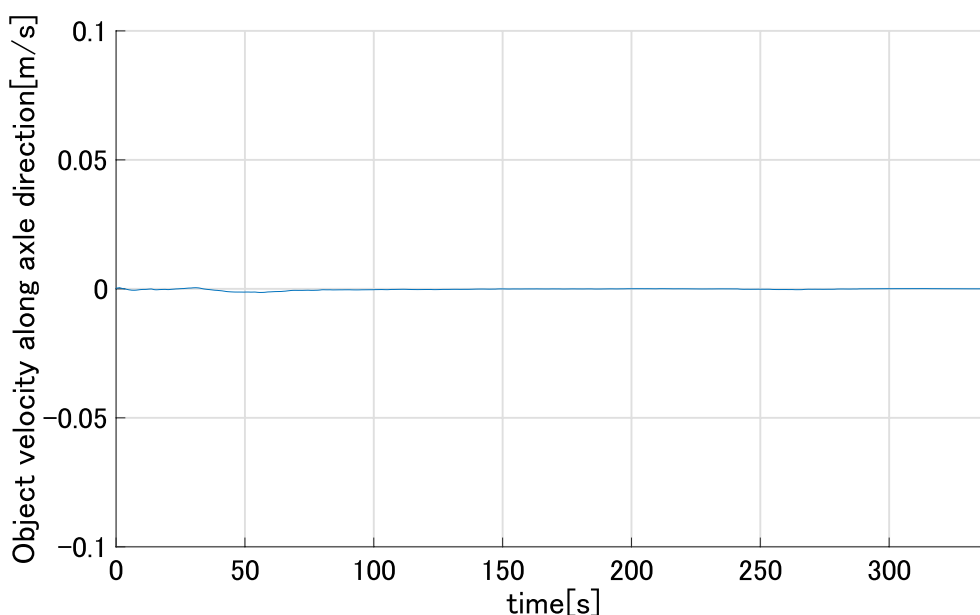


Fig. 18 Object's velocity along the axle direction in the experiment

orientation. The method demonstrated successful performance even when $\theta(0) = 0$ rad.

Additionally, we conducted 10 repeated experiments under the same initial conditions for statistical analysis. The mean time it took for the object to reach the desired position and orientation was 234.35 s, with a standard deviation of 29.11 s. This corresponds to a coefficient of variation (CV) of 0.12, indicating that the object consistently reached the target within a similar timeframe across trials. In many fields, CV value below 0.1 is generally considered to indicate sufficiently small variability [26, 27]. Furthermore, we computed the time-series data of the mean and standard deviation of the object's position and orientation at each time step. We confirmed that the standard deviation was not excessively large, thereby verifying the stability and consistency of the controller.

Conclusion

We proposed a distributed controller for the cooperative transport of an object with two parallel passive fixed wheels by a swarm robot. We conducted the analysis of an object with two parallel passive fixed wheels and derived the center of rotation of the object as a control point of the object. The proposed controller consisted of two steps: step 1 determined the desired velocity and desired angular velocity of the object to reach the desired position and orientation, and step 2 determined the desired velocity of each robot in a distributed manner to achieve the desired velocity and desired angular velocity of the object. We demonstrated the effectiveness of the proposed controller by

confirming that the object reached the desired position and orientation in both the dynamic simulation and real robot experiment.

Future work includes the realization of a controller that reduces the amount of information that the robot needs to acquire, experiments in a distributed experimental system, designing a method based on dynamics considering force, exploring optimal robot formations, investigating strategies for adapting the formation during transportation, and considering a method for any robot failure. Furthermore, while we proposed a method for transporting an object in a distributed manner, we assumed that the robots surround the object and form closure is achieved. It remains a challenge for future work to develop a method for the robots to surround the object in a distributed manner and achieve form closure.

Acknowledgements

Not applicable.

Author contributions

Y.F.: Conceptualization, investigation, methodology, software, experiments, writing-original draft; T.T.: Methodology; T.E. and F.M.: Conceptualization, methodology, supervision, writing-review and editing; Y.M., T.K., and D.M.: Conceptualization, methodology. All authors have read and agreed to the published version of the manuscript.

Data availability

No datasets were generated or analysed during the current study.

Declarations

Ethics approval and consent to participate

Not applicable.

Competing interests

The authors declare no competing interests.

Received: 18 February 2025 Accepted: 1 May 2025

Published online: 24 May 2025

References

- Brambilla M, Ferrante E, Birattari M, Dorigo M (2013) Swarm robotics: a review from the swarm engineering perspective. *Swarm Intell* 7(1):1–41
- Tuci E, Alkilabi MHM, Akanyeti O (2018) Cooperative object transport in multi-robot systems: a review of the state-of-the-art. *Front Robot AI* 5
- Gross R, Mondada F, Dorigo M (2006) Transport of an object by six pre-attached robots interacting via physical links. In: Proceedings of the IEEE international conference on robotics and automation (ICRA). pp 1317–1323
- Wang Z, Schwager M (2016) Force-Amplifying N-robot Transport System (Force-ANTS) for cooperative planar manipulation without communication. *Int J Robot Res* 35(13):1564–1586
- Marino A (2018) Distributed adaptive control of networked cooperative mobile manipulators. *IEEE Trans Control Syst Technol* 26(5):1646–1660
- Verginis CK, Mastellaro M, Dimarogonas DV (2020) Robust cooperative manipulation without force/torque measurements: control design and experiments. *IEEE Trans Control Syst Technol* 28(3):713–729
- Hu J, Liu W, Zhang H, Yi J, Xiong Z (2022) Multi-robot object transport motion planning with a deformable sheet. *IEEE Robot Autom Lett* 7(4):9350–9357
- Kube CR, Hong Z (1993) Collective robotics: from social insects to robots. *Adapt Behav* 2(2):189–218
- Kube CR, Kube CR, Bonabeau E (2000) Cooperative transport by ant and robots. *Robot Auton Syst* 30(1–2):85–101
- Yamada S, Saito J (2001) Adaptive action selection without explicit communication for multirobot box-pushing. *IEEE Trans Syst Man Cybern* 31(3):398–404
- Gerkey BP, Mataric MJ (2002) Pusher-watcher: an approach to fault-tolerant tightly coupled robot coordination. In: Proceedings of the IEEE international conference on robotics and automation (ICRA). pp 464–469
- Fink J, Hsieh MA, Kumar V (2008) Multi-robot manipulation via caging in environments with obstacles. In: Proceedings of the IEEE international conference on robotics and automation (ICRA), pp 1471–1476
- Chen J, Gauci M, Li W, Kolling A, Gross R (2015) Occlusion-based cooperative transport with a swarm of miniature mobile robots. *IEEE Trans Robot* 31(2):307–321
- Ebel H, Eberhard P (2021) Non-prehensile cooperative object transportation with omnidirectional mobile robots: organization, control, simulation, and experimentation. In: Proceedings of the international symposium multi-robot multi-agent system (MRS), pp 1–10
- Ebel H, Luo W, Yu F, Tang Q, Eberhard P (2021) Design and experimental validation of a distributed cooperative transportation scheme. *IEEE Trans Autom Sci Eng* 18(3):1157–1169
- Ebel H, Rosenfelder M, Eberhard P (2024) Cooperative object transportation with differential-drive mobile robots: Control and experimentation. *Rob Auton Syst* 173:104612
- Alkilabi MH, Narayan A, Tuci E (2017) Cooperative object transport with a swarm of e-puck robots: robustness and scalability of evolved collective strategies. *Swarm Intell* 11(3–4):185–209
- Alkilabi MH, Narayan A, Lu C, Tuci E (2018) Evolving group transport strategies for e-puck robots: moving object towards a desired area. In: Proceedings of the international symposium distributed autonomous robotics system (DARS), pp 503–516
- Shibata K, Jimbo T, Matsubara T (2021) Deep reinforcement learning of event-triggered communication and control for multi-agent cooperative transport. In: Proceedings of the IEEE international conference on robotics and automation (ICRA), pp 8671–8677
- Pereira GA, Campos MF, Kumar V (2004) Decentralized algorithms for multi-robot manipulation via caging. *Int J Robot Res* 23(7–8):783–795
- Yoshikawa T, Kurisu M (1991) Identification of the center of friction from pushing an object by a mobile robot. In: Proceedings of the IEEE/RSJ international conference on intelligence robotics system (IROS), pp 449–454
- Sampei M (1994) A control strategy for a class of nonholonomic systems—time-state control form and its application. In: Proceedings of the IEEE conference decision and control (CDC), pp 1120–1121
- Pomet JB (1992) Explicit design of time-varying stabilizing control laws for a class of controllable systems without drift. *Syst Control Lett* 18(2):147–158
- Samson C (1995) Control of chained systems: application to path following and time-varying point-stabilization of mobile robots. *IEEE Trans Autom Control* 40(1):64–77
- Khennouf H, Canudas de Wit C (1996) Quasi-continuous exponential stabilizers for nonholonomic systems. *IFAC Proc* 29(1):2448–2453
- Lu Y-C, Tien Y-M, Juang CH, Lin J-S (2020) Uncertainty of volume fraction in bimrock using the scan-line method and its application in the estimation of deformability parameters. *Bull Eng Geol Environ* 79(3):1651–1668
- Li K (2024) Research on the factors influencing the spatial quality of high-density urban streets: a framework using deep learning, street scene images, and principal component analysis. *Land* 13(8):1161–1186

Publisher's Note

Springer Nature remains neutral with regard to jurisdictional claims in published maps and institutional affiliations.

Yuto Fukao received the B.E. degree in Engineering Science from Osaka University in 2018, and the M.E. degrees in Engineering from Kyoto University in 2020. He is currently a Ph.D. candidate at the Department of Mechanical Engineering and Science, Graduate School of Engineering, Kyoto University, Kyoto, Japan. His research interests include swarm robotics and rescue support systems for fires and disasters.

Tatsuro Terakawa received the B.E. degree in mechanical engineering from Kyoto University, Japan, in 2014, and the M.E. and the Dr. Eng. degrees from Kyoto University Graduate School of Engineering, Department of Mechanical Engineering and Science, in 2016 and 2019, respectively. Since 2019, he has been an Assistant Professor with the Department of Mechanical Engineering and Science, Kyoto University. His research interests include mechanisms and control of wheeled mobile robots, actuator mechanisms, and design. Dr. Terakawa is a member of JSME, JSDE, and RSJ. He received JSME Medals for Outstanding Paper in 2018 and 2024, a JSME Young Engineers Award in 2021, a JSME Miura award in 2016, a JSDE encouragement award in 2018, an IFToMM World Congress Best Application Paper Award in 2019, a JSME MD&T division encouragement presentation in 2016, an FA Foundation paper award in 2019, an FFIT research encouragement award in 2020, and JSAE graduate school research encouragement awards in 2016 and 2019.

Takahiro Endo received the Dr. Eng. degree from the Tokyo Institute of Technology, Tokyo, Japan, in 2006. He was an Assistant Professor at Gifu University, Gifu, Japan, and an Associate Professor at Kyoto University, Kyoto, Japan. Since April 2024, he has been with the Department of Mechanical Engineering, Nagaoka University of Technology, Niigata, Japan, where he is currently a Professor. His research interests include haptics, robotics, and control of infinite-dimensional systems.

Fumitoshi Matsuno received a Dr. Eng. degree from Osaka University in 1986. In 1986, he joined the Department of Control Engineering, Osaka University. He was a Professor in the Department of Mechanical Engineering and Science, Kyoto University from 2009 to 2023. Since 2023 he has been a Professor in Department of Electronics and Information Systems Engineering, Osaka Institute of

Technology, a professor emeritus, Kyoto University, and a deputy director, field of robotics, Fukushima Institute of Research, Education and Innovation (F-REI). He has served as the president of the Institute of Systems, Control, and Information Engineers (ISCIE) and the vice president of the Robotics Society of Japan (RSJ). His research interests include robotics, swarm intelligence and control of nonlinear and distributed parameter systems. He has received awards, including the Best Paper Award from ISCIE in 1986; from the Society of Instrument and Control Engineers (SICE) in 2001, 2006 and 2017; from the Information Processing Society of Japan in 2013; and from the RSJ in 2018, as well as the Prize for Academic Achievement from the Japan Society of Mechanical Engineers (JSME) in 2009 etc. He served as a General Chair of IEEE SSR2011, IEEE/SICE SII2011, SWARM2015, DARS2021 and ASCC2021 etc. He is a Fellow Member of SICE, JSME, RSJ and a senior member of IEEE.

Yoshihiro Morimoto received the B.E and Ph.D. (Dr. Eng.) degree from Tokyo Institute of Technology in 2011 and 2015, respectively. He has been serving as a research engineer at the Advanced Technology R&D Center of Mitsubishi Electric Corporation since April 2015. His primary expertise lies in Robotics, with a focus on Mechanical Engineering.

Takumi Koshimoto received the B.E. degree from Kobe City College of Technology in 2018, and the M.E. degree from Japan Advanced Institute of Science and Technology in 2020. He has been serving as a research engineer at the Advanced Technology R&D Center of Mitsubishi Electric Corporation since April 2020. He has engaged in the research and development of robot control.

Daisuke Mizuno received the B.E and M.E. degrees from Doshisha University in 1998 and 2000, respectively. He joined Mitsubishi Electric Corporation in 2000, where he was responsible for the mechanical design and development of mobile phones. Since 2008, he has been conducting research on mechatronics technology at the Advanced Technology R&D Center. From 2020, he has been serving as the group manager of the Robotics Technology Department.